Predicting an Optimal Oxide/Metal Catalytic Interface for Hydrodeoxygenation Chemistry of Biomass Derivatives

Shyam Deo[*], Michael J. Janik[*1]

[*]Department of Chemical Engineering, The Pennsylvania State University, University Park, Pennsylvania 16802, United States

[1]email: mjj13@psu.edu
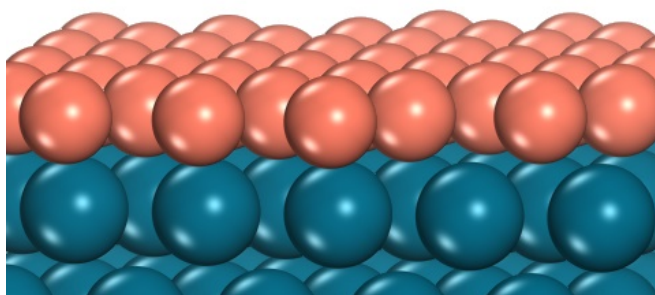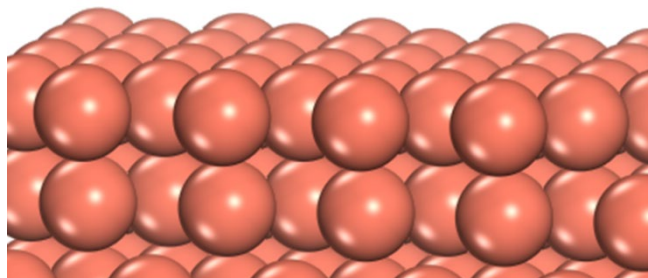
Table of Contents

S1. Surface Models

Figure S1. a) Bare Metal surface, M (111) Model and b) Metal Monolayer over Pd (111) surface, M_{ML}-Pd (111) Model. Color code: Peach color represents a generalized metal M, and dark cyan color represents Pd metal.

S2. Table of Catalytic Descriptors

Table S1. The values of catalytic descriptors work function (Φ), oxygen vacancy formation energy (ΔE_{vac}), metal-carbon binding energy (M-C$_{B.E.}$), and the extent of charge transfer (q) across the interface models. The orange data points represent TiO$_2$/M (111) interface models and blue data points represent TiO$_2$/M$_{ML}$-Pd(111) models where the metals, M forming these interface are indicated.

| S.No.	Metal, M	ΔE_{vac} (eV)	M-C$_{B.E.}$ (eV)	Φ (eV)	q (e$^-$)
1	Ag	3.96	-3.52	4.55	0.15
2	Au	3.52	-4.18	5.27	-0.67
3	Cu	4.00	-6.50	4.46	1.03
4	Rh	3.47	-7.62	4.99	-0.08
5	Ru	3.95	-8.00	4.94	0.42
6	Zn	3.79	-5.69	4.24	1.06
7	Pd	3.04	-7.17	5.20	-0.53
8	Ag	4.35	-3.50	4.76	0.18
9	Au	3.71	-4.22	5.07	-0.64
10	Co	4.37	-6.40	4.25	1.58
11	Cu	4.30	-6.90	4.69	0.91
12	Fe	4.23	-5.82	4.21	2.50
13	Ir	2.37	-8.41	5.89	-0.59
14	Ni	4.15	-5.33	3.98	1.01
15	Pt	2.43	-7.62	5.60	-0.83
16	Rh	3.27	-8.11	5.33	-0.11
17	Ru	3.17	-8.52	5.24	0.21
18	Zn	3.74	-4.68	4.38	1.33
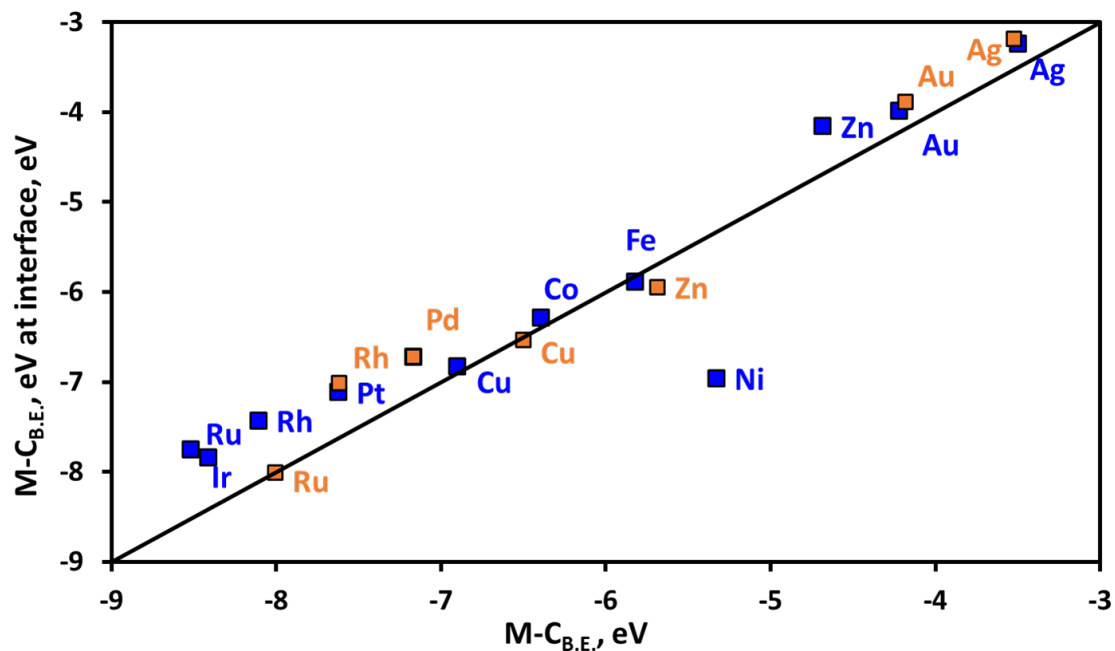
Figure S2. The strong positive correlation of metal carbon-binding energies, M-C$_{B.E.}$ at an interfacial surface vs M-C$_{B.E.}$ over bare M(111) and M$_{ML}$-Pd(111) surfaces (R^2 = 0.86). A parity line is also shown to indicate the deviation between the x and y axis values (mean absolute deviation = 0.41 eV). Orange data points represent TiO$_2$/M(111) interface models and blue data points represent TiO$_2$/M$_{ML}$-Pd(111) models.

S3. Correlation between Catalytic Descriptors

Pearson correlation coefficient, ρ

Pearson's correlation coefficient is defined as the covariance of two variables X and Y divided by the product of their standard deviations. The correlation coefficient ranges from -1 to 1. A value of 1 implies a perfect linear relationship between X and Y, with all data points lying on a line such that Y increases as X increases. Similarly, a value of -1 implies that all data points lie on a line for which Y decreases as X increases. A value of 0 implies that there is no linear correlation between the variables. In addition, either tendency is stronger when the absolute value of the correlation coefficient is larger (for values in between -1 and 1).
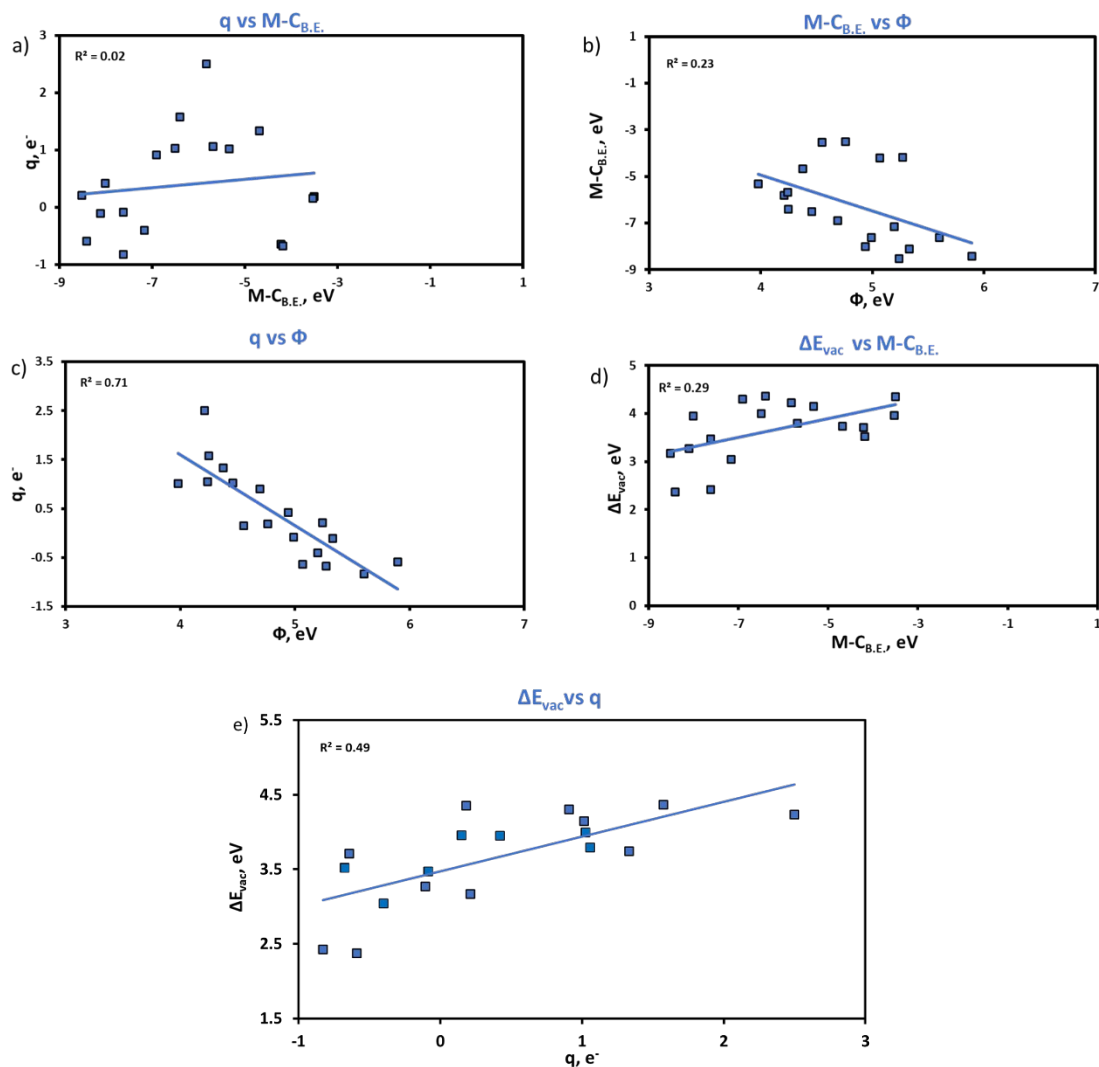
Figure S3. (a-e) Interdependency between the catalytic descriptors work function (Φ), oxygen vacancy formation energy (ΔE_{vac}), metal-carbon binding energy (M-C$_{B.E.}$), and the extent of charge transfer (q) shown by each descriptor plotted against the others. Oxygen vacancy formation energy of the interfacial model, ΔE_{vac} is already plotted against the metal work function, Φ in **Figure 8**.

S4. Energetics for the Dissociative Stability of the Deoxygenation Step

Table S2. Dependence of $\Delta E_{TS\text{-}DDO}$, TS stability for the C-O activation step, S2 (DDO) with respect to bare O deficient surface interface (TiO_{2-x} and gas phase furfuryl alcohol) as defined in equation 5 and the corresponding mean absolute errors (MAE) in eV.

| S. No.	Governing dependence on descriptors (standardized)	R^2	MAE (eV)
1	$\Delta E_{TS\text{-}DDO} = -1.79 + 0.39 \times O_{vac}$	0.57	0.27
2	$\Delta E_{TS\text{-}DDO} = -1.79 + 0.24 \times M\text{-}C_{B.E.}$	0.22	0.37
3	$\Delta E_{TS\text{-}DDO} = -1.79 - 0.48 \times \Phi$	0.85	0.15
4	$\Delta E_{TS\text{-}DDO} = -1.79 + 0.46 \times q$	0.77	0.21
5	$\Delta E_{TS\text{-}DDO} = -1.79 + 0.37 \times O_{vac} + 0.04 \times M\text{-}C_{B.E.}$	0.58	0.27
6	$\Delta E_{TS\text{-}DDO} = -1.79 - 0.04 \times O_{vac} - 0.52 \times \Phi$	0.85	0.15
7	$\Delta E_{TS\text{-}DDO} = -1.79 + 0.14 \times O_{vac} + 0.36 \times q$	0.81	0.21
8	$\Delta E_{TS\text{-}DDO} = -1.79 + 0.01 \times M\text{-}C_{B.E.} - 0.47 \times \Phi$	0.85	0.15
9	$\Delta E_{TS\text{-}DDO} = -1.79 + 0.17 \times M\text{-}C_{B.E.} + 0.43 \times q$	0.88	0.13
10	$\Delta E_{TS\text{-}DDO} = -1.79 - 0.33 \times \Phi + 0.18 \times q$	0.88	0.15
11	$\Delta E_{TS\text{-}DDO} = -1.79 - 0.05 \times O_{vac} + 0.02 \times M\text{-}C_{B.E.} - 0.51 \times \Phi$	0.85	0.15
12	$\Delta E_{TS\text{-}DDO} = -1.79 - 0.03 \times O_{vac} + 0.19 \times M\text{-}C_{B.E.} + 0.45 \times q$	0.88	0.13
13	$\Delta E_{TS\text{-}DDO} = -1.79 - 0.04 \times O_{vac} - 0.36 \times \Phi + 0.18 \times q$	0.89	0.15
14	$\Delta E_{TS\text{-}DDO} = -1.79 + 0.10 \times M\text{-}C_{B.E.} - 0.20 \times \Phi + 0.27 \times q$	0.90	0.13
15	$\Delta E_{TS\text{-}DDO} = -1.79 - 0.10 \times O_{vac} + 0.13 \times M\text{-}C_{B.E.} - 0.25 \times \Phi + 0.30 \times q$	0.91	0.12
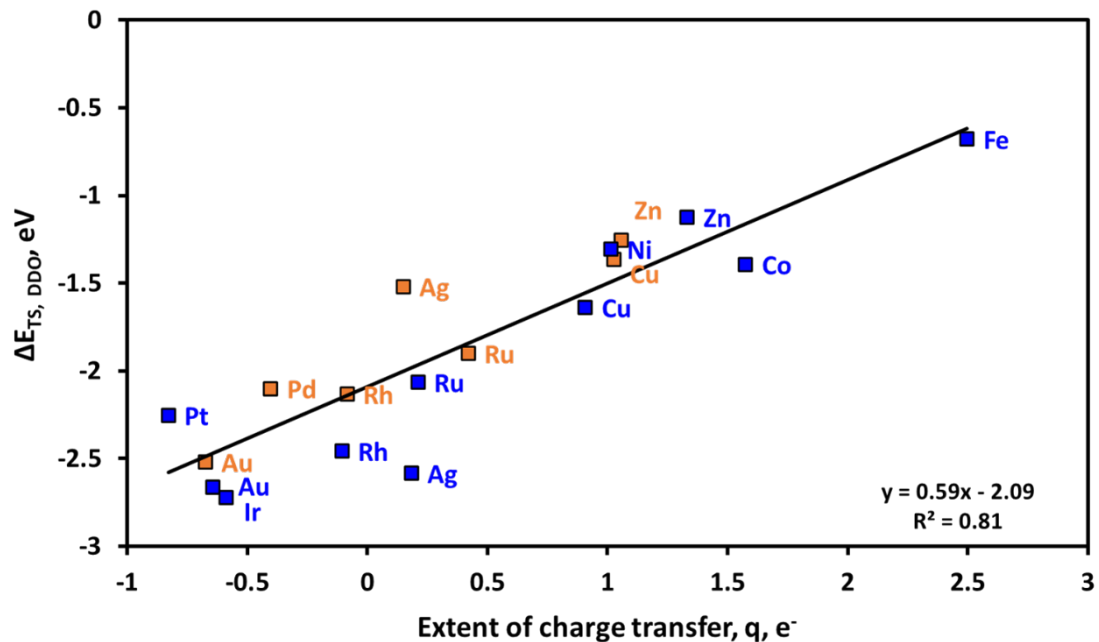
Figure S4. The gas phase stability of the TS state for C-O activation, $\Delta E_{TS,\ DDO}$ vs the extent of charge transfer, q. Orange data points represent TiO_2/M (111) interface models and blue data points represent $TiO_2/M_{ML}-Pd(111)$ models.

S5. Bader charge density difference plots for the C-O activation TS across the TiO_2/M (111) interface model surfaces
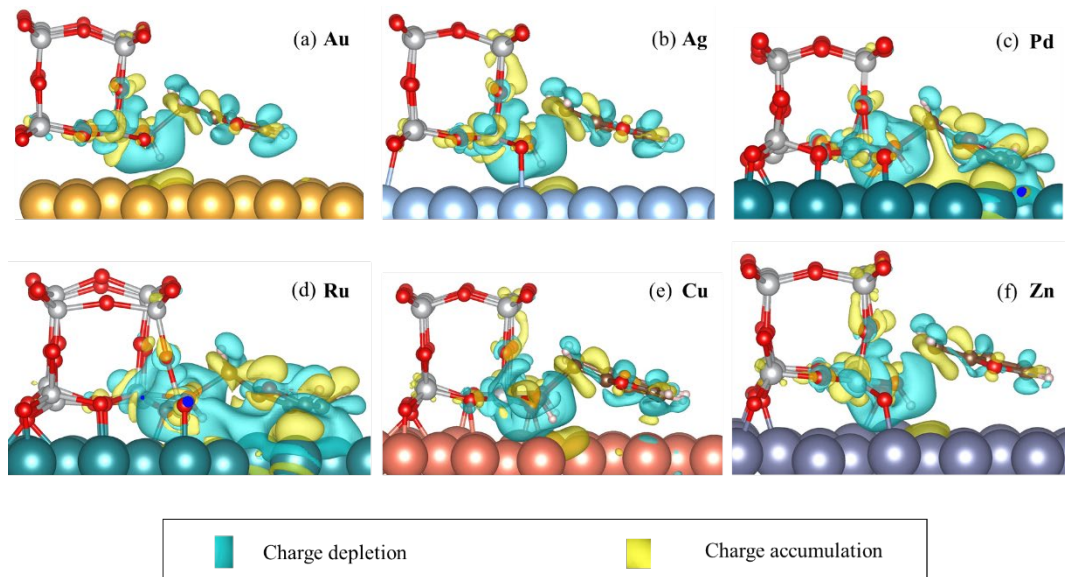

Figure S5. A Bader charge density difference plot during the C-O activation TS over the TiO_2-M (111) interface models where M stands for a) Au, b) Ag, c) Pd, d) Ru, e) Cu and f) Zn. The isosurface level is 0.0013 e Bohr^{-3}. The charge density difference plot is generated through the difference of charge between the DDO transition state structure and separate single-point calculations of the interface and hydrocarbon moieties in the TS structure. The light cyan and yellow colors indicate charge depletion and accumulation, respectively. The Bader charge density difference plot for TiO_2/Rh (111) model surface is already included in **Figure 5b**.

S6. C-H Formation Energetics to the Final Product Methylfuran

Table S3. Dependence of $\Delta E_{TS\text{-}C\text{-}H}$, TS stability for the C-H formation step, S3 relative to bare interface surface (TiO_2/Metal and gas phase furfuryl alcohol) as defined in equation 6 and the corresponding mean absolute errors (MAE) in eV.

S. No.	Governing dependence on descriptors (standardized)	R^2	MAE (eV)
1	$\Delta E_{TS\text{-}C\text{-}H} = -1.49 + 0.68 \times O_{vac}$	0.45	0.62
2	$\Delta E_{TS\text{-}C\text{-}H} = -1.49 + 0.93 \times M\text{-}C_{B.E.}$	0.86	0.30
3	$\Delta E_{TS\text{-}C\text{-}H} = -1.49 - 0.67 \times \Phi$	0.44	0.60
4	$\Delta E_{TS\text{-}C\text{-}H} = -1.49 + 0.40 \times q$	0.16	0.75
5	$\Delta E_{TS\text{-}C\text{-}H} = -1.49 + 0.23 \times O_{vac} + 0.81 \times M\text{-}C_{B.E.}$	0.90	0.23
6	$\Delta E_{TS\text{-}C\text{-}H} = -1.49 + 0.39 \times O_{vac} - 0.33 \times \Phi$	0.49	0.60
7	$\Delta E_{TS\text{-}C\text{-}H} = -1.49 + 0.79 \times O_{vac} - 0.16 \times q$	0.47	0.61
8	$\Delta E_{TS\text{-}C\text{-}H} = -1.49 + 0.80 \times M\text{-}C_{B.E.} - 0.27 \times \Phi$	0.92	0.22
9	$\Delta E_{TS\text{-}C\text{-}H} = -1.49 + 0.89 \times M\text{-}C_{B.E.} + 0.26 \times q$	0.93	0.22
10	$\Delta E_{TS\text{-}C\text{-}H} = -1.49 - 1.15 \times \Phi - 0.57 \times q$	0.53	0.59
11	$\Delta E_{TS\text{-}C\text{-}H} = -1.49 + 0.02 \times O_{vac} + 0.80 \times M\text{-}C_{B.E.} - 0.26 \times \Phi$	0.92	0.22
12	$\Delta E_{TS\text{-}C\text{-}H} = -1.49 + 0.00 \times O_{vac} + 0.89 \times M\text{-}C_{B.E.} + 0.26 \times q$	0.93	0.22
13	$\Delta E_{TS\text{-}C\text{-}H} = -1.49 + 0.40 \times O_{vac} - 0.82 \times \Phi - 0.57 \times q$	0.58	0.58
14	$\Delta E_{TS\text{-}C\text{-}H} = -1.49 + 0.87 \times M\text{-}C_{B.E.} - 0.06 \times \Phi + 0.21 \times q$	0.93	0.22
15	$\Delta E_{TS\text{-}C\text{-}H} = -1.49 - 0.02 \times O_{vac} + 0.88 \times M\text{-}C_{B.E.} - 0.07 \times \Phi + 0.22 \times q$	0.93	0.22

S7. Dissociative Hydrogen Activation Energetics

Table S4. Dependence of $\Delta E_{2H\text{-diss}}$, the dissociative adsorption energy of H_2 relative to bare interface surface (TiO$_2$/Metal and gas phase hydrogen) as defined in equation 7 and the corresponding mean absolute errors (MAE) in eV.

S. No.	Governing dependence on descriptors (standardized)	R^2	MAE (eV)
1	$\Delta E_{2H\text{-diss}} = -0.53 + 0.31 \times O_{vac}$	0.39	0.31
2	$\Delta E_{2H\text{-diss}} = -0.53 + 0.21 \times M\text{-}C_{B.E.}$	0.18	0.37
3	$\Delta E_{2H\text{-diss}} = -0.53 - 0.38 \times \Phi$	0.60	0.28
4	$\Delta E_{2H\text{-diss}} = -0.53 + 0.34 \times q$	0.48	0.31
5	$\Delta E_{2H\text{-diss}} = -0.53 + 0.28 \times O_{vac} + 0.05 \times M\text{-}C_{B.E.}$	0.40	0.30
6	$\Delta E_{2H\text{-diss}} = -0.53 - 0.05 \times O_{vac} - 0.42 \times \Phi$	0.60	0.27
7	$\Delta E_{2H\text{-diss}} = -0.53 + 0.13 \times O_{vac} + 0.25 \times q$	0.52	0.29
8	$\Delta E_{2H\text{-diss}} = -0.53 + 0.03 \times M\text{-}C_{B.E.} - 0.36 \times \Phi$	0.60	0.27
9	$\Delta E_{2H\text{-diss}} = -0.53 + 0.16 \times M\text{-}C_{B.E.} + 0.31 \times q$	0.58	0.28
10	$\Delta E_{2H\text{-diss}} = -0.53 - 0.32 \times \Phi + 0.07 \times q$	0.60	0.28
11	$\Delta E_{2H\text{-diss}} = -0.53 - 0.07 \times O_{vac} + 0.04 \times M\text{-}C_{B.E.} - 0.42 \times \Phi$	0.60	0.27
12	$\Delta E_{2H\text{-diss}} = -0.53 - 0.02 \times O_{vac} + 0.16 \times M\text{-}C_{B.E.} + 0.33 \times q$	0.58	0.28
13	$\Delta E_{2H\text{-diss}} = -0.53 - 0.05 \times O_{vac} - 0.36 \times \Phi + 0.07 \times q$	0.61	0.27
14	$\Delta E_{2H\text{-diss}} = -0.53 + 0.07 \times M\text{-}C_{B.E.} - 0.23 \times \Phi + 0.14 \times q$	0.61	0.27
15	$\Delta E_{2H\text{-diss}} = -0.53 - 0.09 \times O_{vac} + 0.1 \times M\text{-}C_{B.E.} - 0.28 \times \Phi + 0.16 \times q$	0.62	0.27

S8. Correlation of Various Energetics with the Catalytic Descriptors

$$y = 0.56x + 1.85$$
$$R^2 = 0.98$$
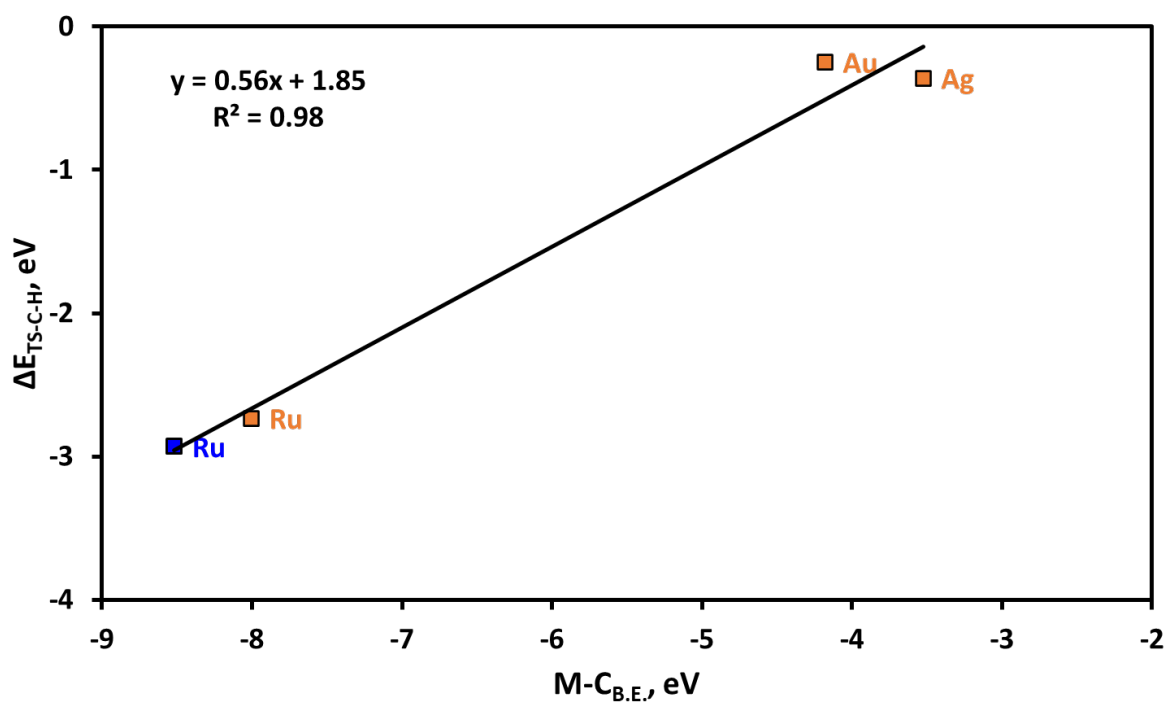
Figure S6. The stability of C-H formation transition state (with O vacancy present at the interface), $\Delta E_{TS\text{-}C\text{-}H}$, is plotted versus the metal carbon binding strength, $M\text{-}C_{B.E.}$ Orange data points represent TiO_2/M (111) interface models and blue data point represents $TiO_2/M_{ML}\text{-}Pd(111)$ model.
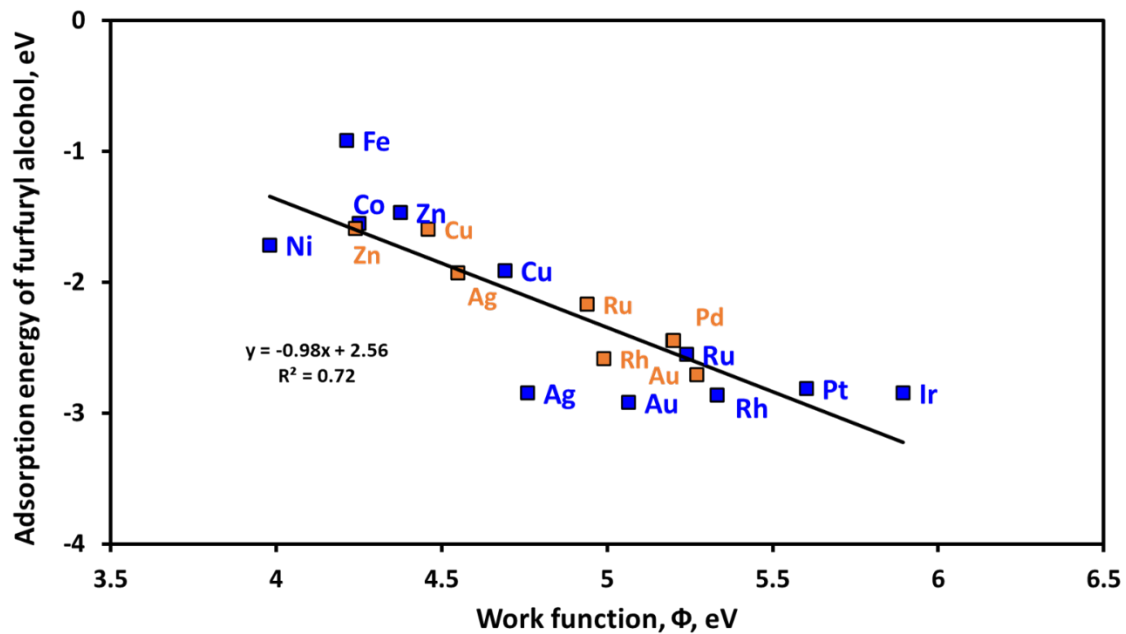
Figure S7. The strong correlation of the adsorption energy of furfuryl alcohol over an interfacial vacancy (initial state (IS) for C-O activation) vs metal workfunction, Φ. Orange data points represent TiO_2/M (111) interface models and blue data points represent TiO_2/M_{ML}-Pd(111) models.
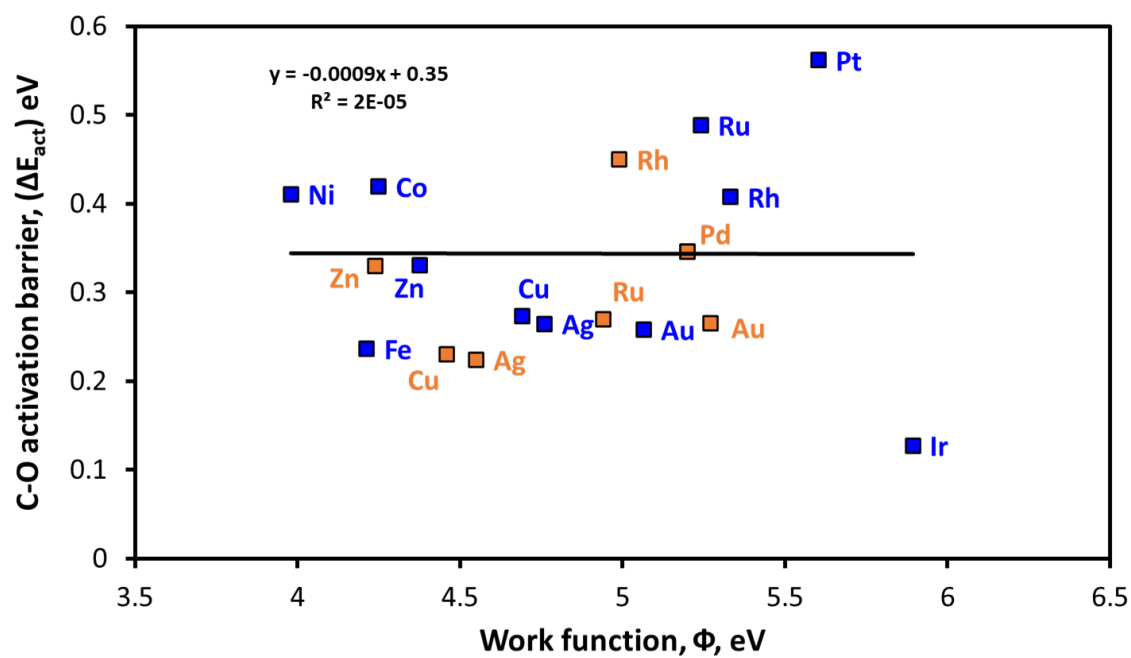
Figure S8. The activation barrier for C-O activation (DDO), ΔE_{act} vs metal workfunction, Φ. Orange data points represent TiO_2/M (111) interface models and blue data points represent TiO_2/M_{ML}-Pd(111) models.
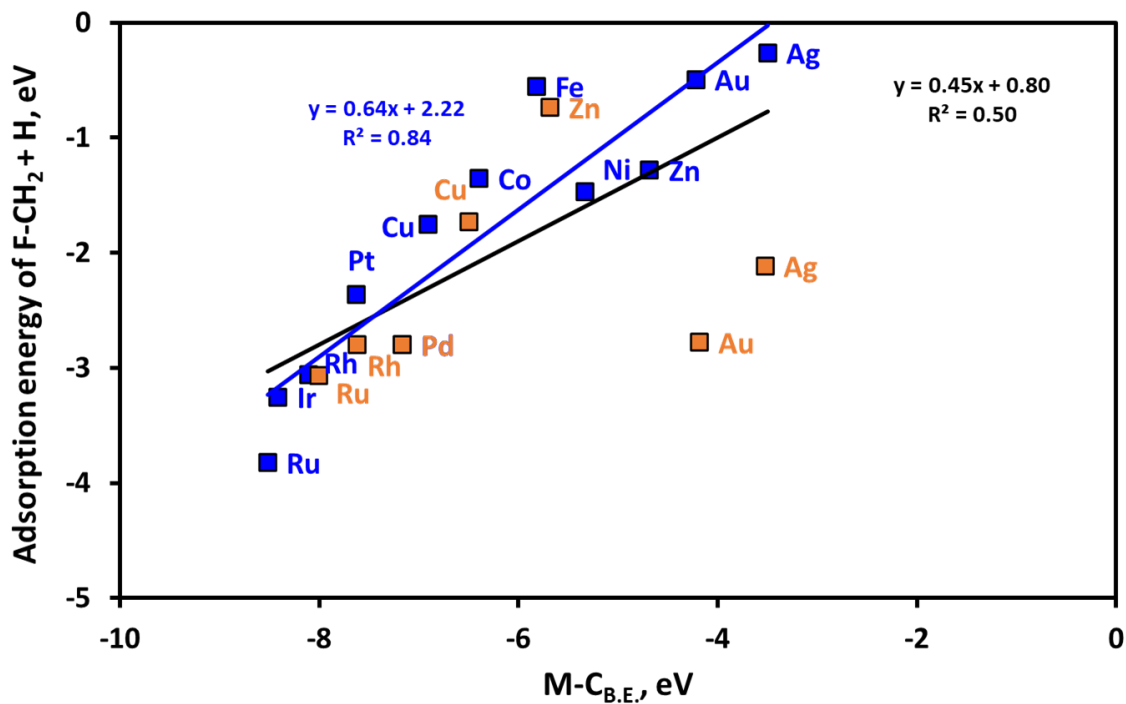
Figure S9. The correlations of the adsorption energy of the F-CH$_2$ + H state over an interfacial vacancy (initial state (IS) for C-H formation) vs metal-carbon binding energy, M-C$_{B.E.}$. F stands for furanic ring. Orange data points represent TiO$_2$/M (111) interface models and blue data points represent TiO$_2$/M$_{ML}$-Pd (111) models. The linear trend (black) shows the combined correlation for the TiO$_2$/M (111) and the TiO$_2$/M$_{ML}$-Pd (111) interface models, while the linear trend (blue) shows the correlation for the TiO$_2$/M$_{ML}$-Pd (111) interface models only.
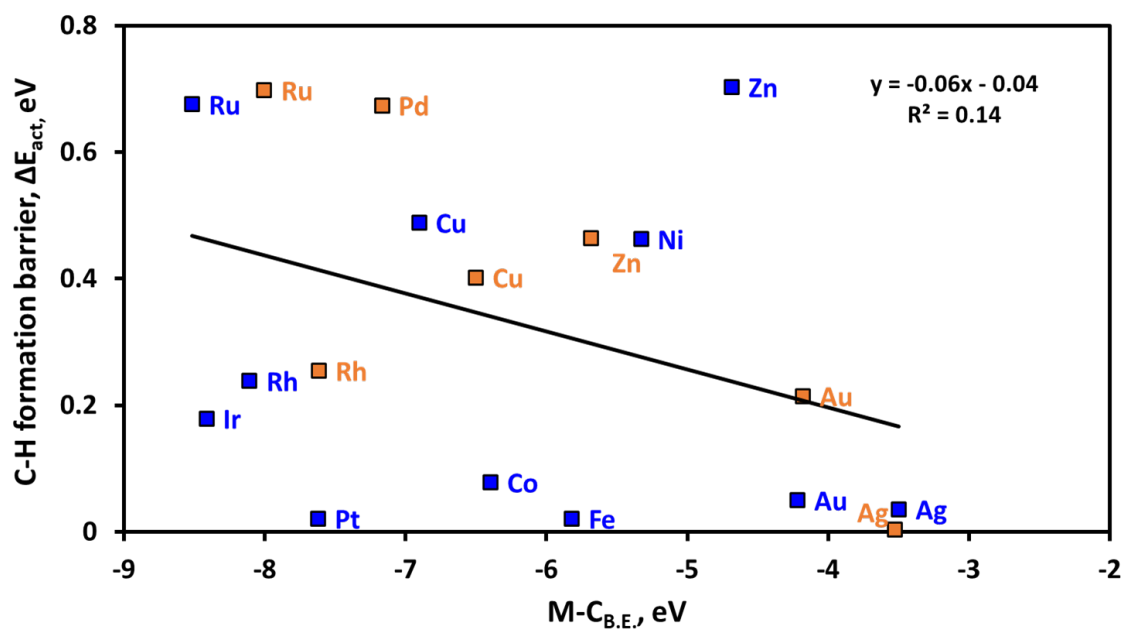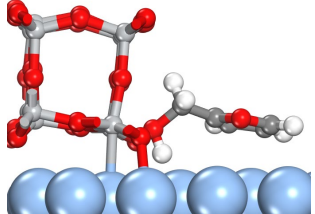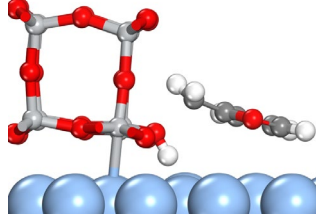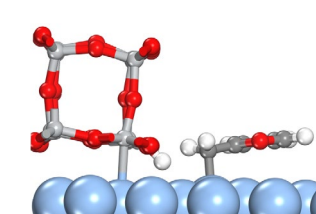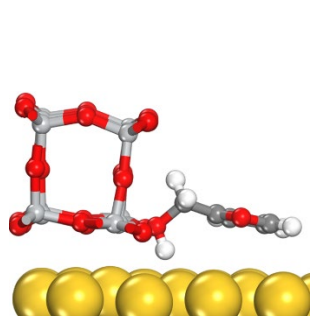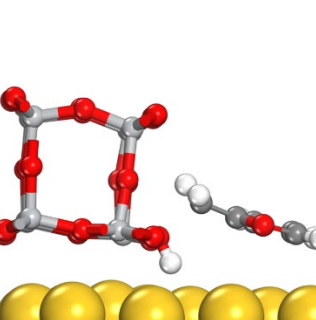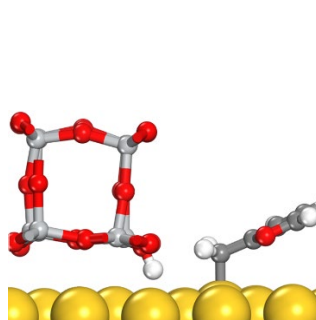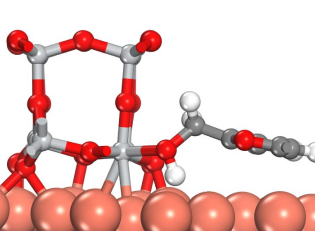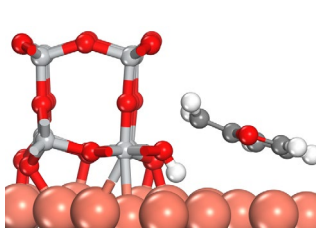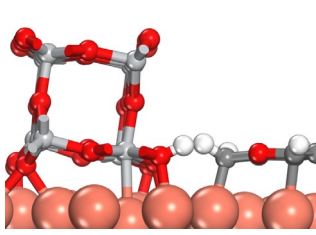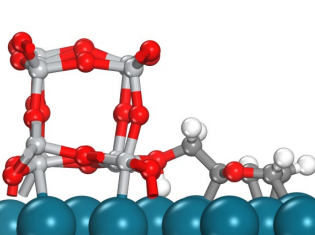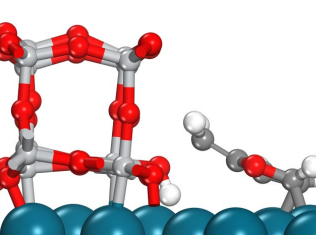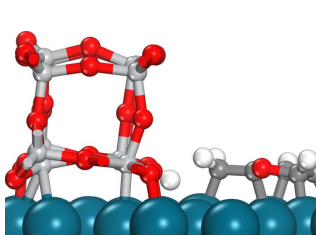
Figure S10. The activation barrier for C-H formation, ΔE_{act} vs metal-carbon binding energy, M-$C_{B.E.}$. Orange data points represent TiO_2/M (111) interface models and blue data points represent TiO_2/M_{ML}-Pd(111) models.

S9. Initial state (IS), transition state (TS) and final state (FS) structures for HDO catalytic steps across the TiO₂/M (111) and the TiO₂/M_ML-Pd (111) interface models.

Table S5. Initial state (IS), transition state (TS) and final state (FS) structures for the C-O activation step across the TiO₂/M (111) and the TiO₂/M_ML-Pd (111) interface models. Color code: gray represents Ti, dark grey represents C, white represents H, red represents O and the fifth color shade represents the metal surface M.

Interface Model	IS	TS	FS
TiO₂/Ag (111)			
TiO₂/Au (111)			
TiO₂/Cu (111)			
TiO₂/Pd (111)			

TiO$_2$/Rh (111)			
TiO$_2$/Ru (111)			
TiO$_2$/Zn (111)			
TiO$_2$/Ag$_{ML}$-Pd (111)			
TiO$_2$/Au$_{ML}$-Pd (111)			
TiO$_2$/Co$_{ML}$-Pd (111)			

TiO$_2$/Cu$_{ML}$-Pd (111)			
TiO$_2$/Fe$_{ML}$-Pd (111)			
TiO$_2$/Ir$_{ML}$-Pd (111)			
TiO$_2$/Ni$_{ML}$-Pd (111)			
TiO$_2$/Pt$_{ML}$-Pd (111)			

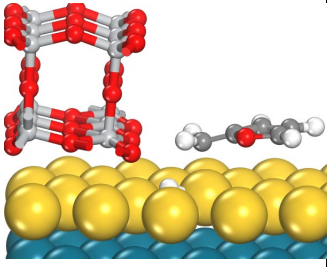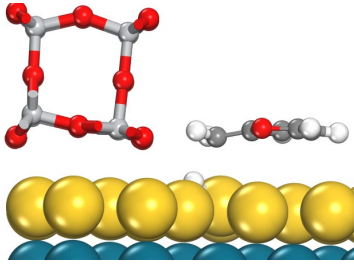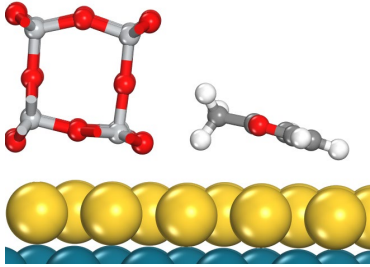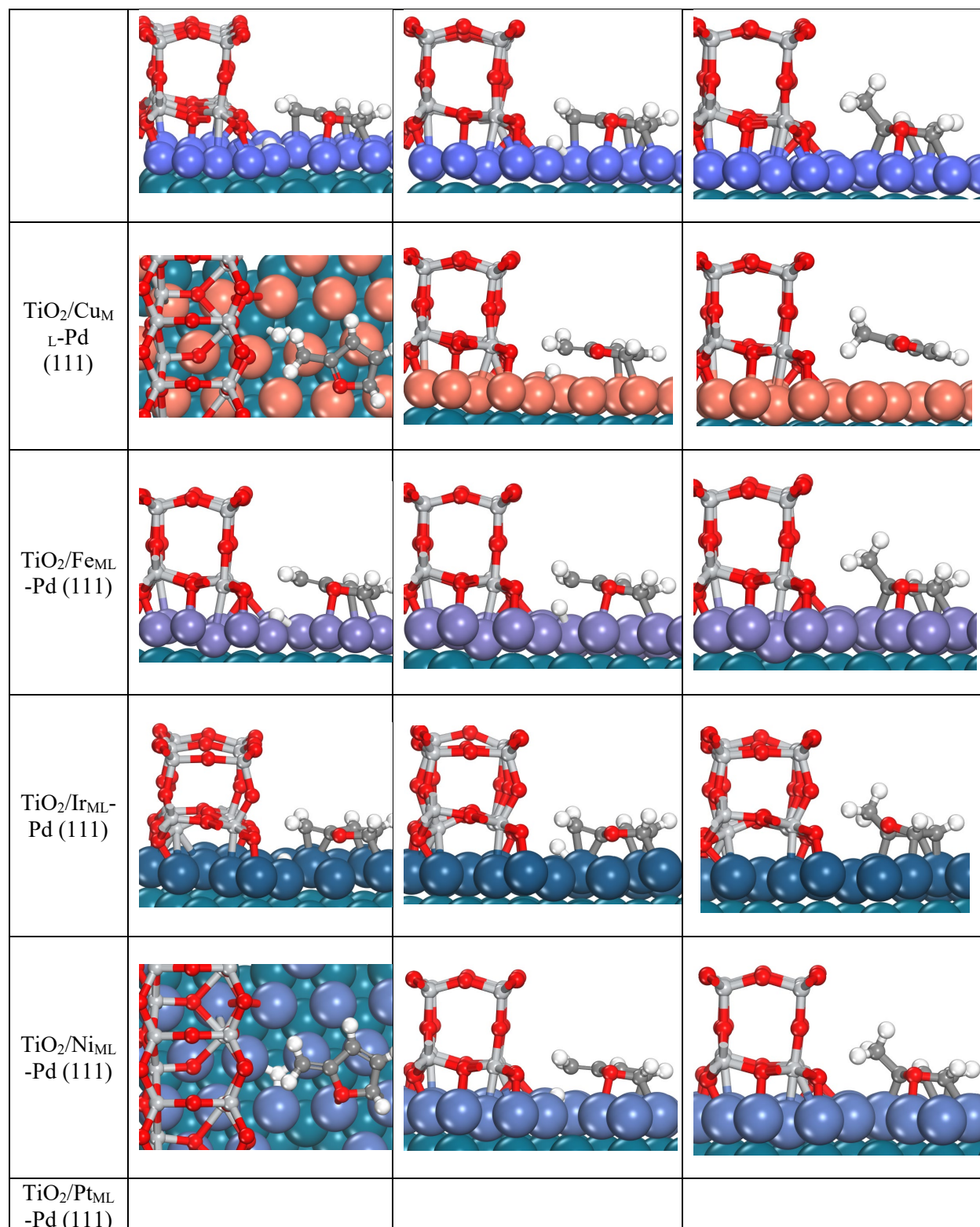|			
TiO$_2$/Rh$_{ML}$-Pd (111)			
TiO$_2$/Ru$_{ML}$-Pd (111)			
TiO$_2$/Zn$_{ML}$-Pd (111)			
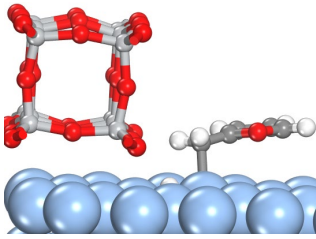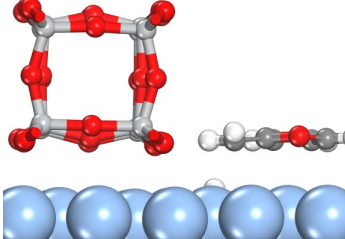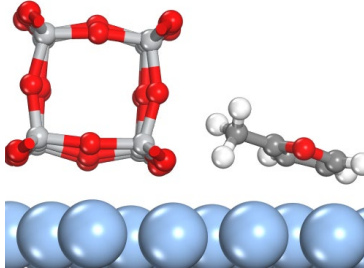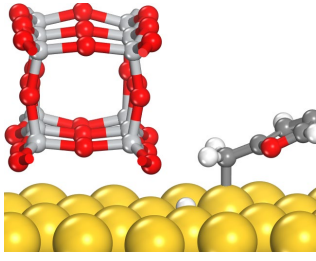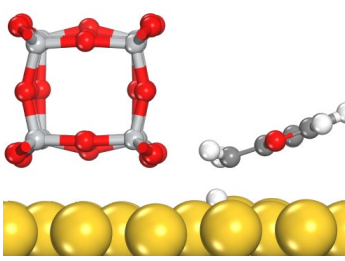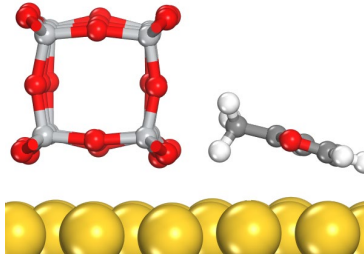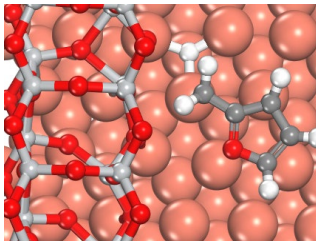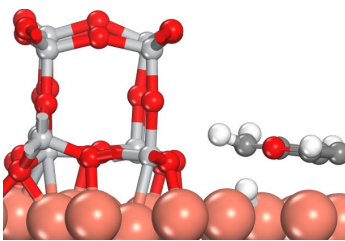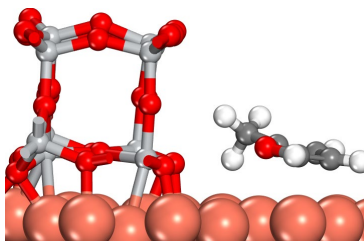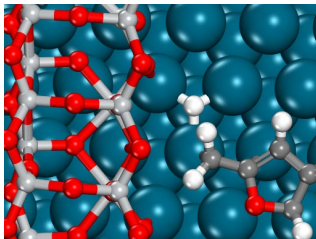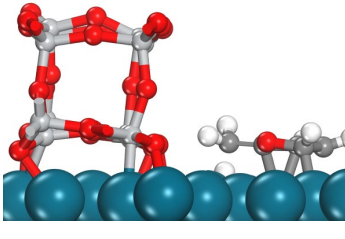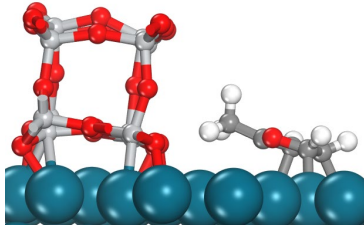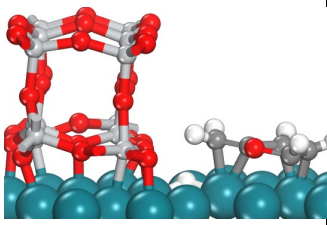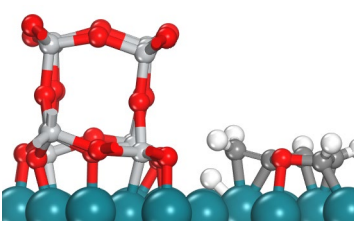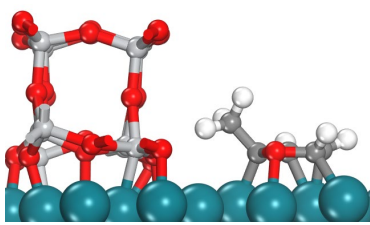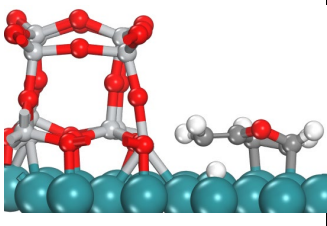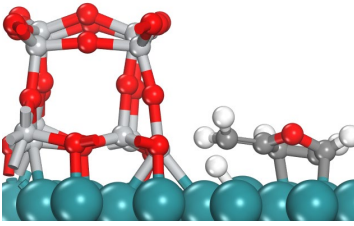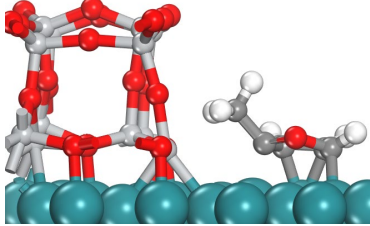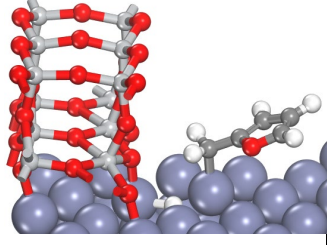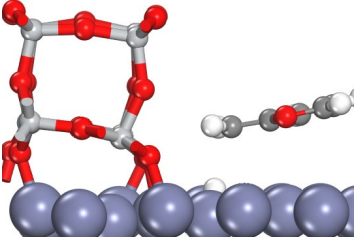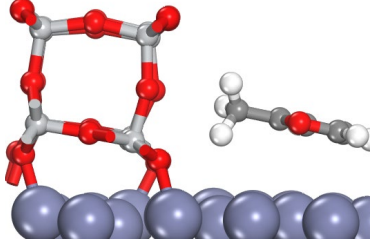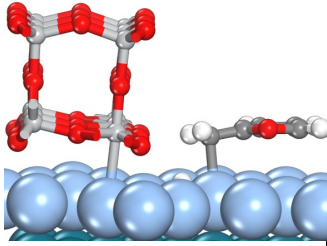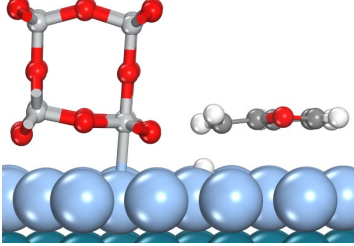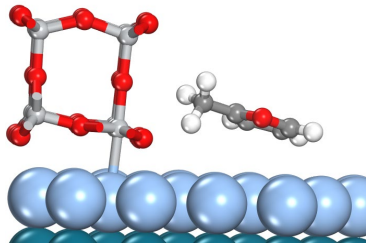
Table S6. Initial state (IS), transition state (TS) and final state (FS) structures for the C-H formation step across the TiO$_2$/M (111) and the TiO$_2$/M$_{ML}$-Pd (111) interface models. Color code: gray represents Ti, dark grey represents C, white represents H, red represents O and the fifth color shade represents the metal surface M.

Interface Model	IS	TS	FS
TiO$_2$/Ag (111)			
TiO$_2$/Au (111)			
TiO$_2$/Cu (111)			
TiO$_2$/Pd (111)			

TiO$_2$/Rh (111)			
TiO$_2$/Ru (111)			
TiO$_2$/Zn (111)			
TiO$_2$/Ag$_{ML}$-Pd (111)			
TiO$_2$/Au$_{ML}$-Pd (111)			
TiO$_2$/Co$_{ML}$-Pd (111)			

TiO$_2$/Cu$_{ML}$-Pd (111)			
TiO$_2$/Fe$_{ML}$-Pd (111)			
TiO$_2$/Ir$_{ML}$-Pd (111)			
TiO$_2$/Ni$_{ML}$-Pd (111)			
TiO$_2$/Pt$_{ML}$-Pd (111)			

TiO$_2$/Rh$_{M L}$-Pd (111)			
TiO$_2$/Ru$_{M L}$-Pd (111)			
TiO$_2$/Zn$_{M L}$-Pd (111)			
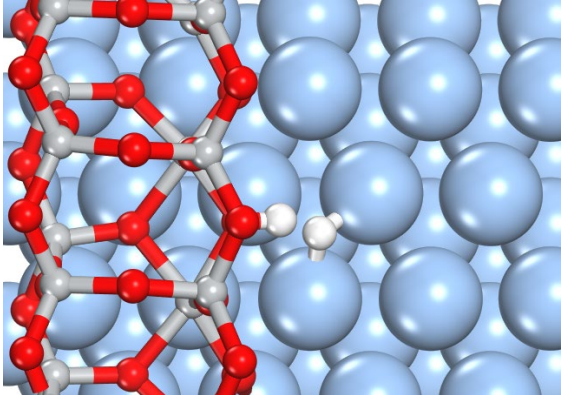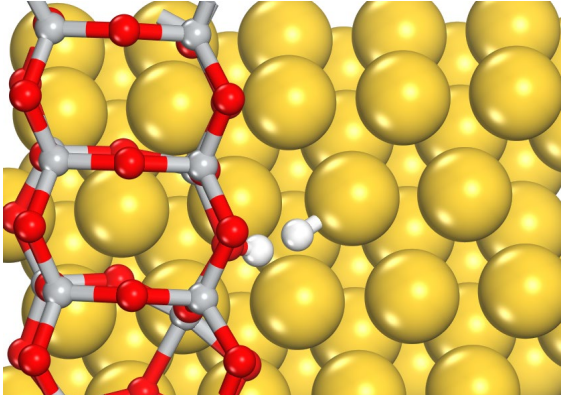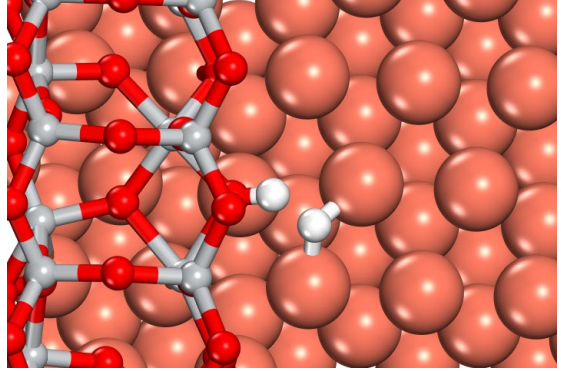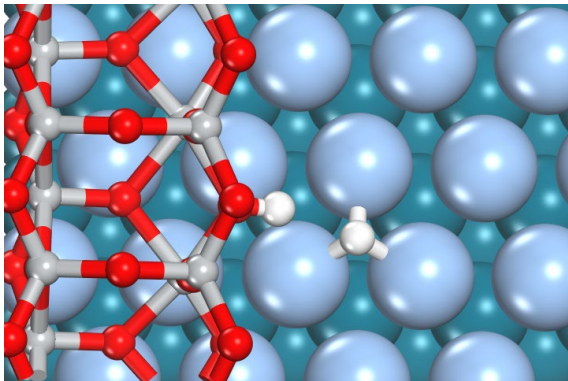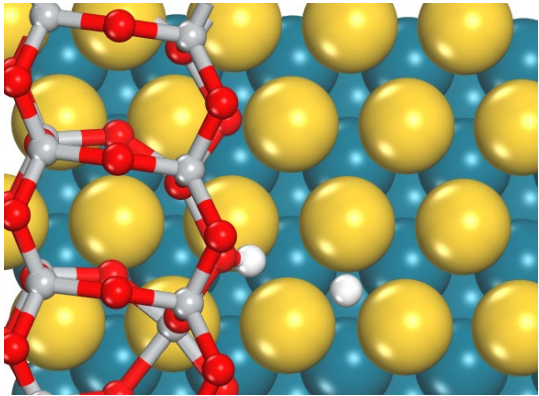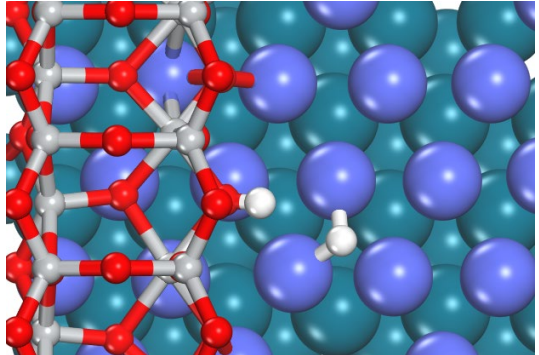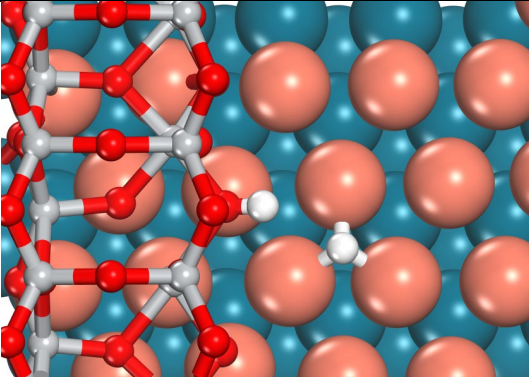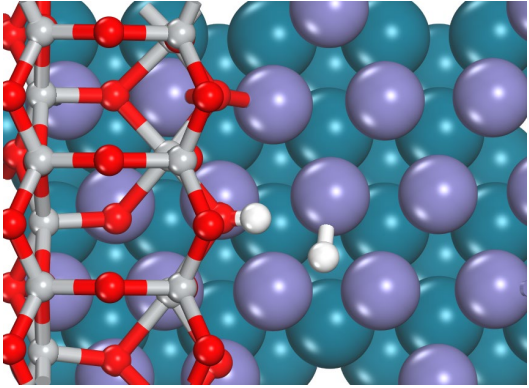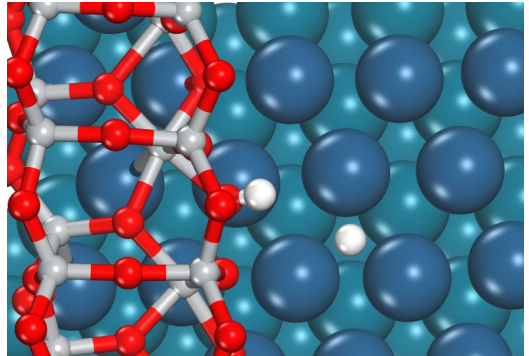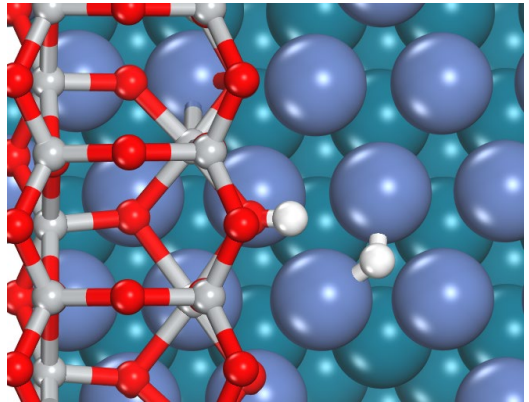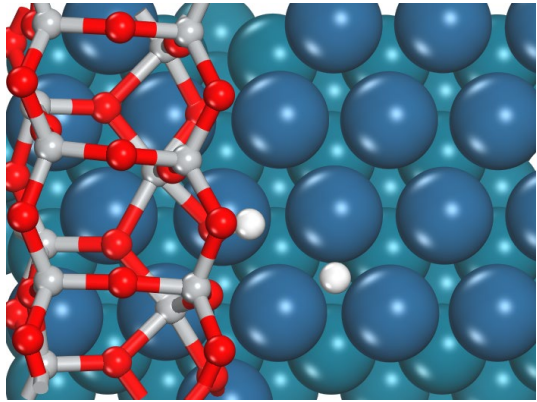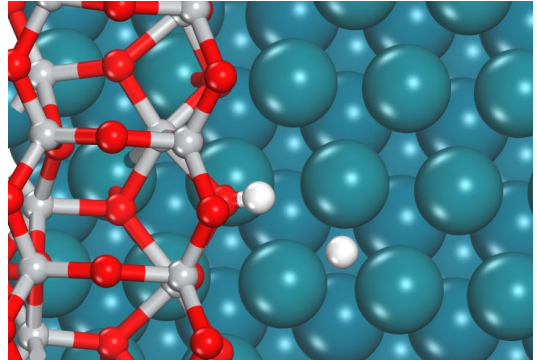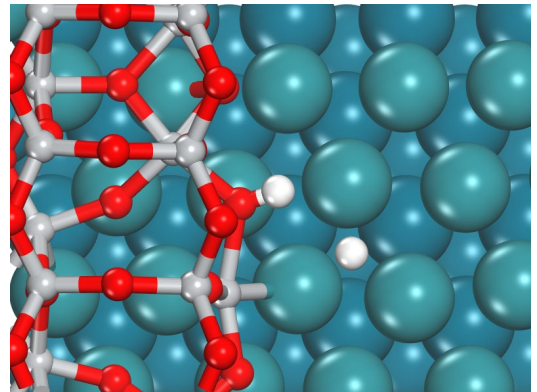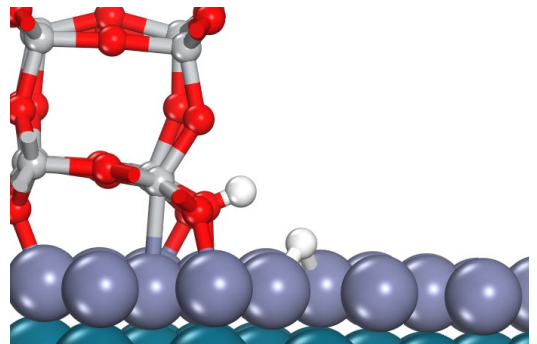
Table S7. The structures for H$_2$ activation/dissociative adsorption across the TiO$_2$/M (111) and the TiO$_2$/M$_{ML}$-Pd (111) interface models. Color code: gray represents Ti, white represents H, red represents O and the fourth color shade represents the metal surface M.

Interface Model	Structure
TiO$_2$/Ag (111)	
TiO$_2$/Au (111)	
TiO$_2$/Cu (111)	
TiO$_2$/Pd (111)	

TiO$_2$/Rh (111)	
TiO$_2$/Ru (111)	
TiO$_2$/Zn (111)	

TiO$_2$/Ag$_{ML}$-Pd (111)	
TiO$_2$/Au$_{ML}$-Pd (111)	
TiO$_2$/Co$_{ML}$-Pd (111)	
TiO$_2$/Cu$_{ML}$-Pd (111)	

TiO$_2$/Fe$_{ML}$-Pd (111)	
TiO$_2$/Ir$_{ML}$-Pd (111)	
TiO$_2$/Ni$_{ML}$-Pd (111)	

TiO$_2$/Pt$_{ML}$-Pd (111)	
TiO$_2$/Rh$_{ML}$-Pd (111)	
TiO$_2$/Ru$_{ML}$-Pd (111)	
TiO$_2$/Zn$_{ML}$-Pd (111)	

S10. HDO Kinetic Analysis

Derivation of rate expressions for the different kinetic regimes

Scenario 1: Interfacial site is highly reducible, and adsorbed hydrocarbon coverage is low.

1a. *If S2 (DDO step) is the rate determining step (RDS).*

From equation 15 we have following:

$$\textbf{HDO rate} = \frac{(K_1.k_2)\ K_3\ K_4\ P_{H_2}\ P_{FAL}}{K_3\ K_4\ P_{H_2} + K_1\ K_3\ K_4\ P_{H_2}\ P_{FAL} + P_{FCH_3}P_{H_2O} + K_3\ P_{H_2O}}$$

where Θ_{Ovac}, $\Theta_{FAL\text{-}vac}$, Θ_{FCH_2} and Θ^*, represent the coverage/concentration of oxygen vacancy (O_{vac}^*), furfuryl alcohol (FAL) adsorbed in a vacancy, organic fragment methylfuryl (FCH_2^*), and stoichiometric TiO_2 interfacial sites (*), respectively from steps S1-S4. These concentrations are determined by each of the four terms in the denominator of the above equation, respectively.

For S2 as the RDS, only the first two terms (Θ_{Ovac} and $\Theta_{FAL\text{-}vac}$) dominate. However, since we have assumed a low hydrocarbon coverage, the hydrocarbon concentrations,

$$\Theta_{FAL\text{-}vac} \ll \Theta_{Ovac}$$

As such, the only term left in the denominator is $K_3\ K_4\ P_{H_2}$ for Θ_{Ovac}. As such, equation 15 reduces to

$$\textbf{HDO rate} = (K_1\ k_2)\ P_{FAL} \qquad\qquad \textit{Scenario 1a, 17}$$

as shown in the main paper.

1b. *If S3 (C-H formation step) is the rate determining step (RDS).*

From equation 16 we have following:

$$\text{HDO rate} = \frac{(K1\ K2)\ k3\ K4\ P_{H2}\ P_{FAL}}{K4\ P_{H2} + K1\ K4\ P_{H2}\ P_{FAL} + K1\ K2\ K4\ P_{H2}P_{FAL} + P_{H2O}}$$

where Θ_{Ovac}, $\Theta_{FAL\text{-}vac}$, Θ_{FCH2} and Θ^*, represent the coverage/concentration of oxygen vacancy (O_{vac}^*), furfuryl alcohol (FAL) adsorbed in a vacancy, organic fragment methylfuryl (FCH_2^*), and stoichiometric TiO_2 interfacial sites (*), respectively from steps S1-S4. These concentrations are determined by each of the four terms in the denominator of the above equation, respectively.

For S3 as the RDS, only the first three terms (Θ_{Ovac}, $\Theta_{FAL\text{-}vac}$ and Θ_{FCH2}) dominate. However, since we have assumed a low hydrocarbon coverage, the terms containing hydrocarbon concentrations,

$$\Theta_{FAL\text{-}vac} \text{ and } \Theta_{FCH2} \ll \Theta_{Ovac}$$

As such, the only term left in the denominator is $K4\ P_{H2}$. As such, equation 15 reduces to

$$\text{\textbf{HDO rate}} = (K1\ K2)\ k3\ P_{FAL} \qquad\qquad \textit{Scenario 1b, 18}$$

as shown in the main paper.

Scenario 2: Interfacial surface is not highly reducible, and adsorbed hydrocarbon coverage is low.

2a. *If S2 (DDO step) is the rate determining step (RDS).*

From equation 15 we have following:

$$\text{HDO rate} = \frac{(K1.k2)\ K3\ K4\ P_{H2}\ P_{FAL}}{K3\ K4\ P_{H2} + K1\ K3\ K4\ P_{H2}\ P_{FAL} + P_{FCH3}P_{H2O} + K3\ P_{H2O}}$$

where similar to scenario 1a & 1b earlier, Θ_{Ovac}, $\Theta_{FAL\text{-}vac}$, Θ_{FCH2} and Θ^*, represent the coverage/concentration of oxygen vacancy (O_{vac}^*), furfuryl alcohol (FAL) adsorbed in a vacancy, organic fragment methylfuryl (FCH_2^*), and stoichiometric TiO_2 interfacial sites (*), respectively from steps S1-S4. These concentrations are determined by each of the four terms in the denominator of the above equation, respectively.

With a less reducible interfacial surface, the concentration of oxygen vacancies, Θ_{Ovac} would be quite low, with higher concentrations of Θ^*. Under low hydrocarbons coverage, the middle two terms from the denominator would also vanish.

As such, the only term left in the denominator is $K3\ P_{H2O}$. The equation 15, therefore, reduces to

$$\text{HDO rate} = \frac{(K1\ k2)\ K4\ P_{H2}\ P_{FAL}}{P_{H2O}} \qquad\qquad \textit{Scenario 2a, 19}$$

as shown in the main paper.

2b. *If S3 (C-H formation step) is the rate determining step (RDS).*

From equation 16 we have following:

$$\textbf{HDO rate} = \frac{(K1\ K2)\ k3\ K4\ P_{H2}\ P_{FAL}}{K4\ P_{H2} + K1\ K4\ P_{H2}\ P_{FAL} + K1\ K2\ K4\ P_{H2}P_{FAL} + P_{H2O}}$$

where Θ_{Ovac}, $\Theta_{FAL\text{-}vac}$, Θ_{FCH2} and Θ^*, represent the coverage/concentration of oxygen vacancy ($O_{vac}{}^*$), furfuryl alcohol (FAL) adsorbed in a vacancy, organic fragment methylfuryl ($FCH_2{}^*$), and stoichiometric TiO_2 interfacial sites (*), respectively from steps S1-S4. These concentrations are determined by each of the four terms in the denominator of the above equation, respectively.

Similar to scenario 2a, for a less reducible interfacial surface, the concentration of oxygen vacancies, Θ_{Ovac} (first term) would be quite low, with higher concentrations of Θ^*. Under low hydrocarbons coverage, the middle two terms from the denominator would also vanish.

As such, the only term left in the denominator is P_{H2O} for Θ^*. And, then equation 16 reduces to

$$\textbf{HDO rate} = \frac{(K1\ K2\ k3)\ K4\ P_{H2}\ P_{FAL}}{P_{H2O}} \qquad\qquad \textit{Scenario 2b, 20}$$

as shown in the main paper.

Scenario 3: Hydrocarbon coverage is high.

3a. *If S2 (DDO step) is the rate determining step (RDS).*

From equation 15 we have following:

$$\text{HDO rate} = \frac{(K1.k2)\ K3\ K4\ P_{H2}\ P_{FAL}}{K3\ K4\ P_{H2} + K1\ K3\ K4\ P_{H2}\ P_{FAL} + P_{FCH3}P_{H2O} + K3\ P_{H2O}}$$

where Θ_{Ovac}, $\Theta_{FAL\text{-}vac}$, Θ_{FCH2} and Θ^*, represent the coverage/concentration of oxygen vacancy (O_{vac}^*), furfuryl alcohol (FAL) adsorbed in a vacancy, organic fragment methylfuryl (FCH_2^*), and stoichiometric TiO_2 interfacial sites (*), respectively from steps S1-S4. These concentrations are determined by each of the four terms in the denominator of the above equation, respectively.

With S2 as the RDS, only the first two terms (Θ_{Ovac} and $\Theta_{FAL\text{-}vac}$) dominate. Under high hydrocarbon coverage, the hydrocarbon concentrations $\Theta_{FAL\text{-}vac} \gg \Theta_{Ovac}$. As such, the only term left in the denominator is $K1\ K3\ K4\ P_{H2}\ P_{FAL}$ for this term. As such, equation 15 reduces to

$$\text{HDO rate} = k2 \qquad\qquad \textit{Scenario 3a, 21}$$

as shown in the main paper.

3b. *If S3 (C-H formation step) is the rate determining step (RDS).*

From equation 16:

$$\textbf{HDO rate} = \frac{(K1\ K2)\ k3\ K4\ P_{H2}\ P_{FAL}}{K4\ P_{H2} + K1\ K4\ P_{H2}\ P_{FAL} + K1\ K2\ K4\ P_{H2}P_{FAL} + P_{H2O}}$$

where Θ_{Ovac}, $\Theta_{FAL\text{-}vac}$, Θ_{FCH2} and Θ^*, represent the coverage/concentration of oxygen vacancy (O_{vac}^*), furfuryl alcohol (FAL) adsorbed in a vacancy, organic fragment methylfuryl (FCH_2^*), and stoichiometric TiO_2 interfacial sites (*), respectively from steps S1-S4. These concentrations are determined by each of the four terms in the denominator of the above equation, respectively.

With S3 as the RDS, only the first three terms (Θ_{Ovac}, $\Theta_{FAL\text{-}vac}$ and Θ_{FCH2}) dominate. Further, under high hydrocarbons coverage, $\Theta_{Ovac} \ll \Theta_{FAL\text{-}vac}$, Θ_{FCH2}. As such, the middle two terms left in the denominator. As such, equation 16 reduces to

$$\textbf{HDO rate} = \frac{(K1\ K2)\ k3\ K4\ P_{H2}\ P_{FAL}}{K1\ K4\ P_{H2}\ P_{FAL}(1+K2)} = \frac{K2\ k3}{(1+K2)} \qquad\qquad \textit{Scenario 3b, 22}$$

Now, if C-O bond activation energetics are also favorable, then K2 >> 1. Then the equation reduces to

$$\textbf{HDO rate} = k3 \qquad\qquad \textit{Scenario 3b, 22}$$

However, if K2 << 1, but C-H bond formation (S3 step) remains the RDS. Then the HDO rate reduces to K2 k3.